BioCore Exploring Scientific Community

International Journal of Nanotechnology in Medicine & Engineering

ISSN 2474-8811

Research Article Open Access

Synthesis, Characterisation and Photoelectrochemical Studies of Graphite/Zinc Oxide Nanocomposites with the Application Exfoliated Electrodes for the Degradation of Methylene Blue

O.M. Ama*, O.A. Arotiba

Department of Applied Chemistry, University of Johannesburg, South Africa.

Corresponding Author: O.M. Ama, Department of Applied Chemistry, University of Johannesburg, P.O. Box 17011, Doornfontein, 2028, South Africa. **Email:** onoyivwe4real@gmail.com

Citation: O.M. Ama et al. (2017), Synthesis, Characterisation and Photoelectrochemical Studies of Graphite/Zinc Oxide Nanocomposites with the Application Exfoliated Electrodes for the Degradation of Methylene Blue. Int J Nano Med & Eng. 2:8, 133-139. DOI:10.25141/2474-8811-2017-8.0145

Received: September 06, 2017; **Accepted:** September 19, 2017; **Published:** September 29, 2017

Abstract:

The search for electrochemically robust materials for electrochemical application in water treatment; we present the preparation of exfoliated graphite which exhibits good electro-photocatalytic propertyand ZnO which possesses high oxygen evolution potential electrodes for the electrochemical degradation of organic pollutants in water. ZnO was prepared by a homogeneous co-precipitation method followed by the preparation of ZnO-exfoliated graphite (EG) electrode. The EG-ZnO electrode was characterized by electron microscopy, Raman spectroscopy, X-ray diffractometry, X-ray photoelectron spectroscopy and electrochemistry. The results showed a good dispersion of the ZnO in the EG and improved potential hole. The EG-ZnO electrode was employed for the electrochemical oxidation of methylene blue dye in synthetic wastewater. The efficiency of degradation was measured by uv-visible spectroscopy and total organic carbon (TOC). The electrode exhibited a higher photodegradation efficiency than the bare EG. The kinetics of this electrochemical reaction was studied using the Langmuir Hinshelwood model. Aside the importance of advance oxidation processes as an alternative or complementary water treatment method, this novel electrode is cheap, easy to prepare and has a robust electrochemistry

Keywords: Exfoliated, Graphit, ZnO, Electrode, TOC

Introduction:

A decreased water quantity and quality is a risk for both humans and the environment. This decreased water quality is nowadays caused by drought, an increasing human population and growing industrial activities. Moreover, the limited amount of potable water accessible for these different demands is ever more concentrated with pollutants. For example, textile industries are generating large quantities of coloured effluents containing organic dyes, surfactants and traces of metals which lead to environmental problems when discharged into water [Sarkar, et al., 2010: Carmen, et al., 2012].

Conventional methods of water treatments such as activated carbon adsorption, membrane filters, ion exchange, coagulation/flocculation and oxidation had been adopted for the treatment polluted or wastewater [Parvathi, et al., 2010]. However, analysis of the water samples treated by these methods often reveals sustained contamination of the water after applying a specific treatment. A further quest for an alternative or complementing treatment methods then brings forth Advanced Oxidation Processes (AOPs) which have been testified to remove organic pollutants, including dyes which occur in wastewater[Chan et al., 2011].

There has been a number of researchers' that employed AOPs, particularly photoelectrochemical degradation method in the degradation of organic pollutants in water. However, most of these works focused on TiO2 and WO3 as the main photocatalyst [Kim et al. 2015: Reyes et al, 2013], with limited work done using zinc oxide (ZnO). Zinc oxide gained greater importance recently based on its excellent optical and electrical properties. These properties make ZnO an appropriate catalyst for potential application in many fields including its use in optical devices and electrochemical capacitor electrodes [Venugopal et al.,2012: Minaee et al ., 2013], oxygen sensor [Lee et al., 2016], fuel cells [Loh et al., 2012], photocatalysis [Loh et al., 2012]] and advance ceramics [Soltani et al., 2014]. Furthermore, the nanocomposite proved its potential in removing dyes efficiently in previous papers when suspended in solution [Daneshvar et al., 2007, Kumar et al., 2016].

This work investigates the degradation capacity of ZnO and exfoliated graphite/Zinc oxide nanocomposite electrodes. The second component of the electrode EG is intended to improve the degradation capacity of ZnO. As a low density carbon material EG

has certain unique properties including its stability to aggressive media, large specific surface area and flexibility. EG is also known to be a good photosensitizer and will therefore enhance the visible light absorption capacity of the electrons. It also has the potential of accepting photogenerated electrons from the ZnO thereby reducing electron-hole recombination [Kumar et al.,2013]. The EG/ZnO photoelectrode is expected to possess excellent photoelectrochemical degradation properties as it is expected to possess synergic properties of both ZnO and EG.

Experimental

Materials and apparatus

All the chemicals used in the experiment were purchased from Sigma-Aldrich. They were of analytical reagent grades and used without further purification. Characterization was carried out using scanning electron microscopy (SEM) alongside energy-dispersive X-ray spectroscopy microanalysis (VGA3 TESCAN), Brunauer–Emmett–Teller (BET) nitrogen adsorption–desorption (Shimadzu, Micromeritics ASAP 2010 Instrument), UV–Vis diffuse reflectance spectroscopy (Shimadzu 2450) of dry powders using $BaSO_4$ as a reflectance standard, X-ray diffractometer (Bruker D8 with Cu-Kα), and Raman spectroscopy (Lab RAM HIR, HoridaJobinXvon, France using 514.5 nm air cooled with Ar+Laser) with ×50 objective and laser intensity of 1.3 mW, New Port 9600 Full Spectrum Solar Simulator equipped with a 400-W ozone-free xenon lamp which produces a collimated beam of 33-mm diameter (equivalent to 1.3 sun).

The experiments were conducted using a photoreactor with approximate volume of 100 mL. The working electrodes used were EG and EG-ZnO with 1 cm2 area, while Ag/AgCl (3.0 M KCl) and platinum foil were used as a reference and a counter electrode respectively. The power supply for electrochemical degradation of methylene blue dye (60 mL) in 0.1 M sodium sulphate supporting electrolyte, a potentiostat/galvanostatic with a voltage range of 1-3 V and a current range of 7.5–15 mA was employed. A 250 W quartz Tungsten-halogen (QTH) lamp equipped with liquid filter was employed to produce a light at the outside surface of the lamp with intensity of 0.27 W. There was a distance of 2 cm between the light source and the reactor. In addition, at 20 min intervals, Aliquots were withdrawn from the electrochemical cell. To study the dye concentration, a UV-Vis spectrophotometer (Perkin Elmer model Lambda 35) was used. Absorption bands at 310 nm were selected for converting the absorbance to concentration using linear regression: $y = 8.5\ x + 0.13667$ obtained from a plot of absorbance vs. concentration (0- 0.8 mM).

Synthesis of ZnO

Zinc sulfate (2 g) was dissolved in 100 mL deionized water and the solution stirred magnetically for 1 hr. Sodium hydroxide solution (3 M) was added drop-by-drop to the solution under vigorous stirring until pH 10 by which time the ZnO precipitate was formed. The stirring was continued for overnight. The precipitate obtained was filtered and washed thoroughly with deionized water. The precipitate was dried in an oven at 100 °C and crushed to powder using mortal and [Gnanasangeetha et al., 2013]. The powder obtained was calcined at 500 °C

Fabrication of EG/ZnO nanocomposites electrode

EG/ZnO nanocomposite material was processed into pellet, which was then used for the fabrication of electrode. Glass rod, copper wire and conducting silver paint were used in the fabrication process.

Results and Discussion

Morphological studies of graphite/Zinc Oxide nanocomposite (SEM/EDS and TEM analysis)

The SEM micrograph of the graphite studied (Fig1a) showed an orientation of layered structures with different sizes. The morphology of the graphitized carbon was observed to be the same irrespective of the orientation or the magnification. The layered structure and the flaky morphology of graphite is due to its molecular structure which fits into its hexagonal crystallography [Jaszczak et al., 1995]. The micrograph in Fig 1 b, shows that ZnO has been synthesized on the graphite, as structures which seem like particles or flower grains are seen covering the flaky layered structure of the graphite.

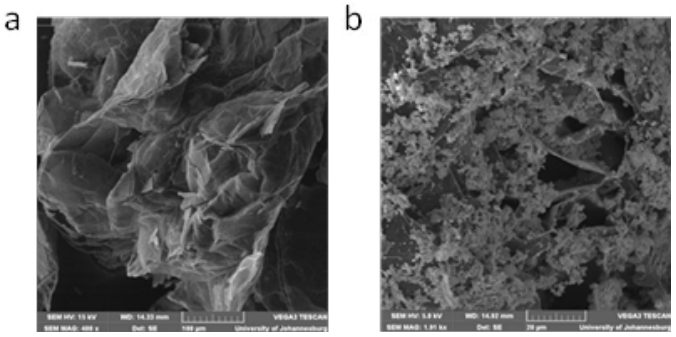

Figure1: SEM micrographs of (a) Graphite (b) EG/ZnO

TEM analysis was carried out to confirm that ZnO was actually synthesized and Fig 2 shows the TEM micrographs obtained from the analysis. The TEM images show irregular hexagonal crystalline structures in nanometers sizes similar to those observed by [Salem et al., 2009]. The TEM micrograph of EG/ZnO (Fig 2) shows clusters of particles in their nano sizes but larger than ZnO in size. The EDX spectrum of the EG/ZnO (Fig 3) also confirmed that ZnO was synthesized and successfully dressed on the graphite. This is seen from the results, which show the presence of Zn, C and O.

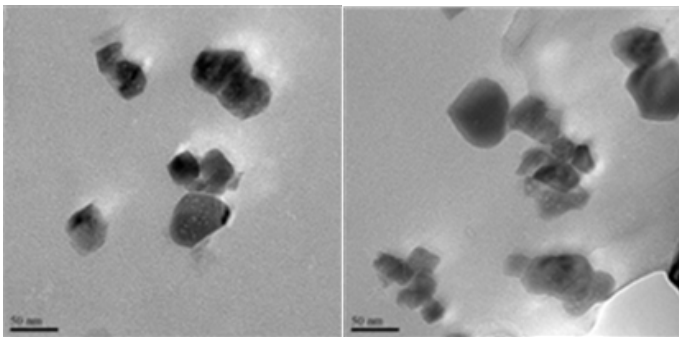

Figure 2: TEM image of (a) ZnO and (b) EG-ZnO materials

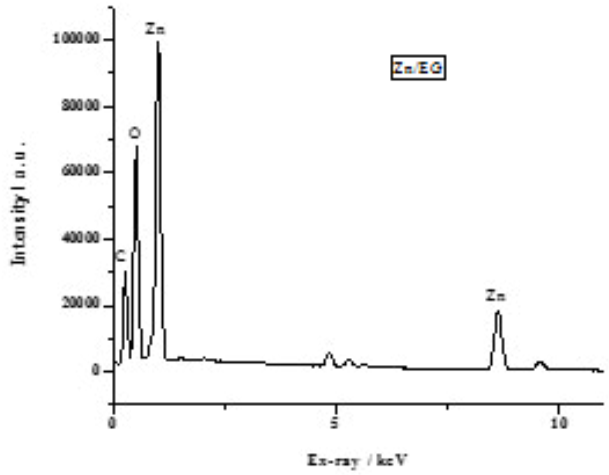

Figure 3: EDX micrograph of EG/ZnO

Raman analysis

Raman spectra of ZnO and EG/ZnO are shown in Fig 4. The Raman spectrum of ZnO is dominated by peaks between 100 and 600 cm^{-1}. The peak found at 476 cm^{-1} is assigned to E_2 (high) mode, while the mode at 186 cm^{-1} is assigned as $2E_2$ (low) [Guo et at., 2009]. In the bulk ZnO spectrum the peak at 378 cm^{-1} corresponds to A1TO and LO-phonon peak is seen in the spectrum of ZnO at 106 cm^{-1}. The mode at 560 cm^{-1} in the Raman spectrum of ZnO is attributed to B1 (high) due to inelastic neutron scattering measurements [Das et al., 2008]. An intrinsic mode of ZnO assigned to transverse acoustic phonon (TA) and longitudinal optical phonons (LO) is found at 642 cm^{-1}.

The spectrums for ZnO Fig 4 (a) do not show D and G-peaks but the D and G-peaks are seen on the EG/ZnO spectrum. This is because these peaks are typical of carbon base materials [Ntsendwana et at., 2016]. EG/ZnO spectrum shows typical D-peak at 1338 $cm^{-1}$and G-peak at 1560 cm^{-1}. The G peak is results from bond stretching of sp^2 carbon pairs in both chains and rings and it corresponds to optical E_2g phonons at the Brillouin zone center [Ntsendwana et at., 2016]. The D peak usually results from the breathing mode of aromatic rings and this can be activated by a defect. Other peaks present on the EG/ZnO spectrum between 100 and 650 cm-1 are from ZnO. The peak corresponding to E_2 high is seen at 438 cm^{-1}.

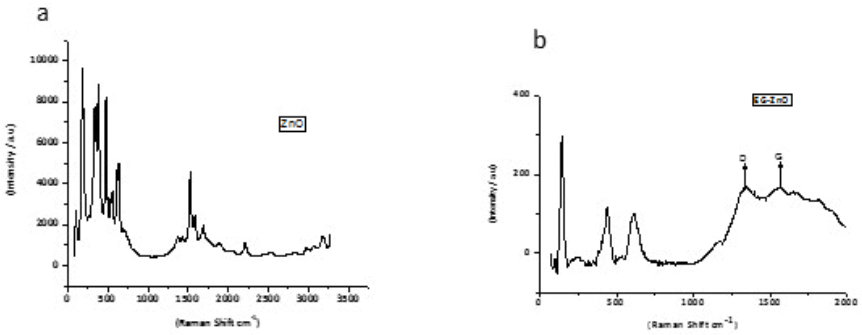

Figure 4: Raman spectra of (a) ZnO (b) EG/ ZnO materials

XRD analysis

The XRD patterns of ZnO and EG/ZnO are shown in Fig 5. The diffraction peaks from the ZnO correspond to the hexagonal Zincite and ZnO structures. The XRD results show that ZnO sample contains majorly the Zincite (crystalline ZnO) with peaks indexed at 31.54º (100), 34.12º (002), 35.98º (101), 47.15º (102), 56.16º (110), 62.30º (103), 65.85º (200), 67.38º (112), 68.53º (201) and 76.29º (202), respectively. These peaks are similar to those observed by Kumar and Rani (Kumar et al.,2013). On the other hand, EG/ZnO contains Zincite, ZnO and majorly carbon that come from the graphite. ZnO are seen at peaks 36.43, 42.32, 61.39, 73.54 and 77.39 o. These peaks correspond to (1,1,1), (2,0,0), (2,2,0), (3,1,1) and (2,2,2) planes, respectively. Peaks corresponding to these planes are also found on the ZnO XRD spectrum. Carbon peaks from graphite are present at 26.40 (0,0,2), 42.31 (1,0,0), 44.48 (1,0,1), 50.56 (1,0,2), 54.36 (0,0,4), 59.68 (1,0,3), 71.20 (1,0,4) and 77.37 (1,1,0).

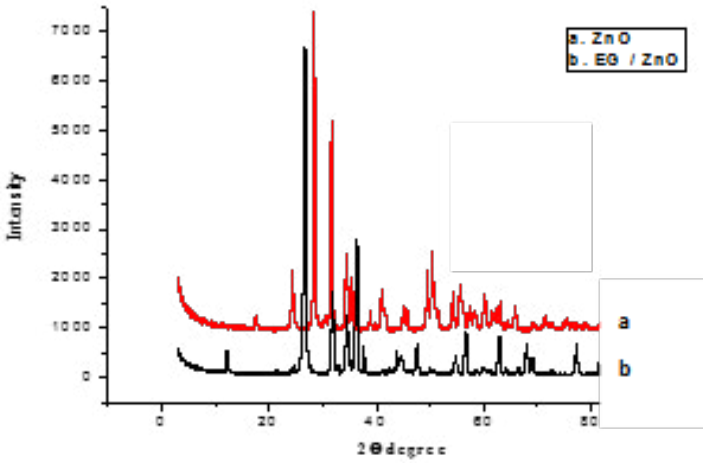

Figure 5: XRD pattern of (a) ZnO and (b) EG-ZnO materials.

BET analysis

The surface areas and pore volumes of EG, ZnO and EG/ZnO are presented in Table 1. The results show that incorporation of ZnO on EG greatly reduced the surface area of EG as well as its pore volume, which indicates that ZnO penetrated into the graphite's pore volume which is larger than that of ZnO. This resulted to lower pore volumes for EG/ZnO electrode [Bott et at., 1999].

Table: 1 BET data of EG, ZnO and EG- ZnO

Sample	BET Surface Area/m^2g^{-1}	Pore Volume/cm^3g^{-1}
EG	10.76	0.0488
ZnO	8.30	0.0562
EG/ ZnO	4.96	0.0258

Electrochemical Characterization of the EG and EG- ZnO

The cyclic voltammograms of EG and EG/ZnO in 5 mM Fe (CN)6 $^{-4}$are shown in Fig 6 According to the results, incorporation of ZnO into EG caused an increase in the current as a result of relatively larger surface area of the EG/ZnO.

The separation of redox potential peaks ΔE_p for EG and EG/ZnO were -0.12V, -0.16V and -0.08V, respectively and the ratio of peak current (Ipa/Ipc) were 1.16, 1.21 and 1.23, respectively. The Ipa/Ipc value is usually 1 (unity), but in this study, it is observed to be deviated from 1 for the three electrodes. These deviations from unity could be attributable to a subsequent chemical reaction that is triggered by the electron transfer [An et al., 2004]. Also, the higher ΔE_p value for EG/ZnO are characteristic of slow electron transfer kinetic. The values of formal potential E_f calculated as the average of cathodic and anodic peak potentials for EG, and EG/ZnO were 0.23 V, 0.24 V and 0.23 V, respectively.

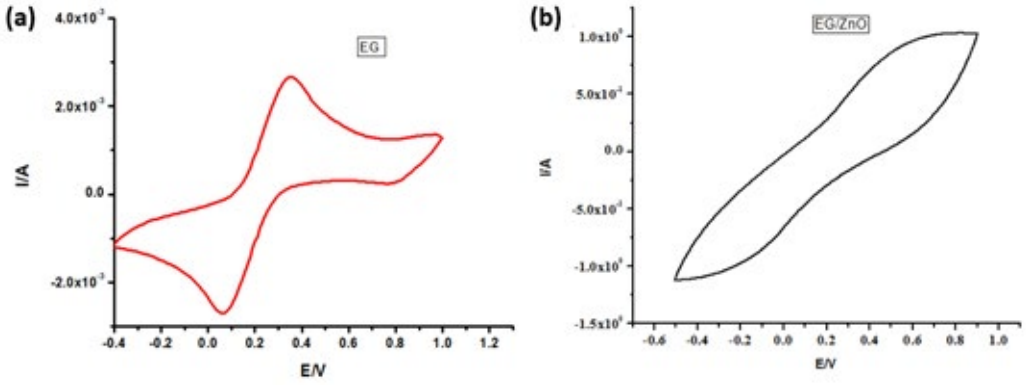

Figure 6: Cyclic voltammograms of (a) EG, and (b) EG/ZnO electrodes in 5 mM $[Fe(CN)6]^{-3/-4}$ at 20 mV s^{-1} (b)

Photoelectrochemical degradation

The UV-Vis of diffuse reflectance spectra of ZnO and EG/ZnO are shown in Fig 7. The ZnO showed optical absorption at about 278 nm. After incorporating ZnO into EG, there was a shift in optical absorption edges to about 373 nm. This means that incorporation of ZnO into EG enhanced the visible light absorption of ZnO. The removal of the methylene blue dye was studied using visible spectrophotometer and the spectra obtained are seen in Fig 8a. The EG and EG modified electrodes (EG/ZnO) were used for the photoelectrochemical degradation of methylene blue dye and the results obtained are presented in Figure 8b. A removal efficiency of 95 % was achieved with EG/ZnO electrode after 180 min, while a removal efficiency of 76% was achieved with EG electrode. Other methods used for methylene blue dye degradation using EG/ZnO in comparison with photoelectrochemical were photolysis and electrochemical oxidation. The photoelectrochemical to be the most suitable method as 95% degradation of methylene blue dye was observed at 180 min. A degradation or removal efficiency of 16% and 19% were observed for photolysis and electrochemical methods, respectively.

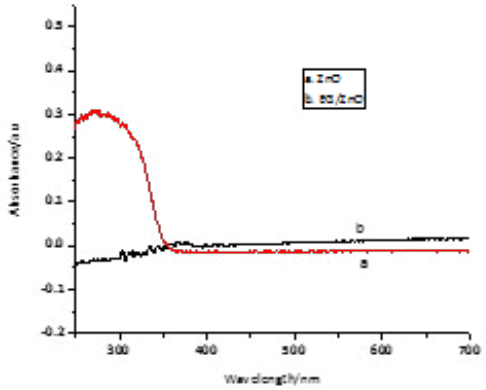

Figure 7: The UV-Vis diffuse reflectance spectra of (a) ZnO and (b) EG- ZnO

The photoelectrochemical oxidation of EG and EG/ZnO photoelectrode towards the degradation of methylene blue dye was investigated using three electrochemical methods electrochemical, photolysis and photoelectrochemical. This process involves adsorption of OH- group on the active surface of the electrode before formation of hydroxyl radicals. The adsorbed OH- groups may react to form oxygen molecules, thus, resulting to oxidation of pollutants at the surface of the electrode leading to low removal efficiency of the pollutant. Electron–hole recombination could be responsible for the lowest performance of photolysis method. According to An et al. [An et al., 2004], oxygen released by electrochemical method can be reproduced as the electron acceptor for oxidation during photolysis process, which further promotes the degradation rate by indirect oxidation (i.e oxidants are formed on the anode before the oxidation process commences).

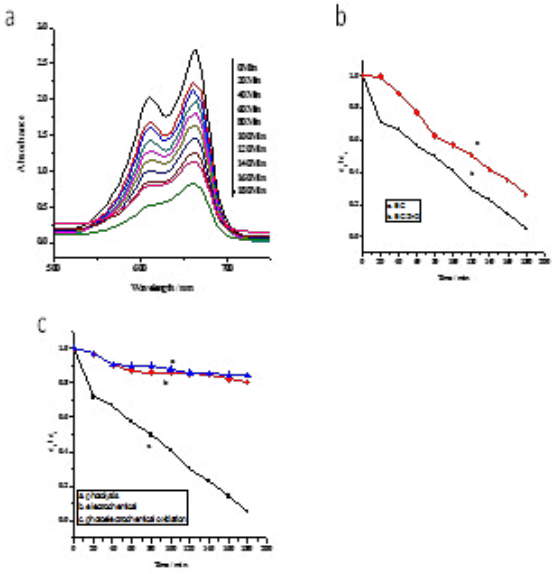

Figure: 8 (a) UV-Vis spectra showing degradation of methylene blue in the first 180 mins (b) Normalized concentration decay curve for the photoelectrochemical degradation of Methylene Blue on (i) EG (ii) EG-ZnO (c) Normalized concentration decay curve for (i) photolytic (ii) electrochemical and (iii) photoelectrochemical degradation of [Methylene blue] and degradation of 0.1×10^{-4} M

A pseudo first-order reaction kinetics ($\ln C_0/C_t = kt$) was used to study the kinetics of the electrodes. In this equation, Co/Ct is the normalized concentration, t is the reaction time, and k is the apparent reaction rate constant. The k values for the photoelectrochemical method for EG and EG/ZnO were observed to be 9.29 x $10^{-1}$and 2.97 min^{-1}, respectively. This shows that EG/ZnO electrode will degrade methylene blue faster than EG electrode. Meanwhile, the k values for the electrodes for electrochemical EG and EG/ZnO as well as electrodes for photolysis for the EG and EG/ZnO were 5.50 x 10^{-2}, 1.86 x 10^{-1}, 3.15 x 10^{-2} and 2.30 x 10^{-1} min^{-1}, respectively.

Table: 2 Values of Rate constant for the Degradation of Methylene Blue

Sample	K (min^{-1})
Photoelectrochemical EG/ZnO	2.9790
Photoelectrochemical EG	0.9293
Electrochemical EG/ZnO	0.1858
Electrochemical EG	0.0550
Photolysis EG/ZnO	0.2295
Photolysis EG	0.0315

Conclusions

Methylene blue degradation using EG and EG/ZnO electrodes was achieved. The EG/ZnO electrode showed better degradation ability compared to EG electrode with an efficiency of 96% using photoelectrochemical method. Amongst the three methods used, photoelectrochemical was found to be more efficient in degradation of methylene blue. The degradation process followed the first-order kinetic as linear relationship was obtained for a plot of concentration ratio against time.

References

1. Sarkar, A., 2010. Emissions Trading and Sustainable Energy Development, Asia Pacific Business Review, 6 42-66.

Carmen, Z., Daniela, S., 2012. Textile organic dyes-characteristics, pollution effects and separation/elimination procedures from industrial effluents- a critical overview, Intech Open Science, 55-81

2. Parvathi, C., Maruthavanan, T., Prakash, C., Koushik, C.V., 2010. Decolouration of dye house effluent by activated carbon, The Indian Textile Journal,

Chan, S.H.S., Yeong, Wu, T., Juan, J.C., The, C.Y., 2011. Recent developments of metal oxide semiconductors as photocatalysts in advanced oxidation processes (AOPs) for treatment of dye waste-water, Journal of Chemical Technology and Biotechnology, 86 1130-1158.

3. Kim, D.H., Bokare, A.D., Koo, M.S., Choi, W., 2015. Heterogeneous catalytic oxidation of As(III) on nonferrous metal oxides in the presence of H_2O_2, Environmental Science and Technology, 49 3506-3513.

4. Reyes, K.R., Robinson, D.B., WO3/TiO2 2013 Nanotube photoanodes for solar water splitting with simultaneous wastewater treatment, Sandia Report, 1-37.

5. Venugopal, N., Yang, B.C., Ko, T., 2012. ZnO/CNT nanocomposite electrode for aqueous electrochemical supercapacitor, Materials Research Innovations 16 96-100.

6. Minaee, H., Mousavi, S.H., Haratizadeh, H., De Oliveira, P.W., 2013. Oxygen sensing properties of zinc oxide nanowires, nanorods, and nanoflowers: The effect of morphology and temperature, Thin Solid Films, 545 8–12.

7. Lee, S.L., Ho, L.N., Ong, S.A., Wong, Y.S., Voon, C.H., Khalik, W. F., Yusoff, N. A., Nordin, N., (2016), Enhanced electricity generation and degradation of the azo dye reactive green 19 in a photocatalytic fuel cell using ZnO/Zn as the photoanode, Journal of Cleaner Production, 127 579–584.

8. Loh L., Dunn S., 2012. Journal of Nanoscience and Nanotechnology,Recent progress in ZnO-based nanostructured ceramics in solar cell applications, 12 8215-8230.

9. Soltani, R. D.C., Rezaee, A., Khataee, A.R., Safari, M., 2014. Photocatalytic process by immobilized carbon black/ZnO nanocomposite for dye removal from aqueous medium: optimization by response surface methodology, 20 1861–1868.

10. Daneshvar, N., Rasoulifard, M.H., Khataee, A.R., Hosseinzadeh, F., 2007Removal of C.I. acid orange 7 from aqueous solution by UV irradiation in the presence of ZnO nanopowder, Journal of Hazardous Materials, 143 95–101.

11. Kumar, P., Sharma, V., Singh, N., Sharma, D., Shrivastav, R., Satsangi, V.R., Dass, S., 2016. Photoelectrochemical splitting of water to produce a power appetizer Hydrogen: A green system for future – A short review, Oriental Journal of Chemistry, 32 1473-1483.

12. Kumar, S. S., Venkateswarlu, P., Rao, V. R., Rao, G. N., 2013. Synthesis, characterization and optical properties of zinc oxide nanoparticles. International Nano Letters, 3 1-6.

Gnanasangeetha, D., SaralaThambavani, D., 2013. One pot synthesis of zinc oxide nanoparticles via chemical and green method. Journal of Material Sciences 2320-6055.

13. [15] Jaszczak, J.A., 1995. Graphite: flat, fibrous and spherical. In Mesomolecules 161-180

14. Salem, J.K., Hammad, T.M., Harrison, R.G., (2009. ZnO nanoparticles prepared in the presence of additives by thermal decomposition. International Journal of Nanoscience, 8465–472.

15. Guo, S., Du, Z., Dai, S., 2009. Analysis of Raman modes in Mn-doped zno nanocrystal, Physica Status Solidi (B), 246 2329–2332.

16. Das, A., Chakraborty, B., Sood, A. K., 2008. Raman spectroscopy of graphene on different substrates and influence of

defects, Bulletin of Material Science, 31 579-584.

17. Ntsendwana, B., Sampath, S., Mamba, B. B., Oluwafemi, O. S., Arotiba, O. A., 2016. Photoelectrochemical degradation of eosin yellowish dye on exfoliated graphite–ZnO nanocomposite electrode, Journal of Material Science and Material Electron 27:592–598.

18. Bott, A.W., 1999. Characterization of chemical reactions coupled to electron transfer reactions using cyclic voltammetry, Current Separations 18 9-16.

19.An, T., Zhang, W., Xiao, X., Sheng, G., Fu, J., Zhu, X., 2004. Photoelectrocatalytic degradation of quinoline with a novel three-dimensional electrode-packed bed photocatalytic reactor, Journal of Photochemistry and Photobiology A: Chemistry, 161 233-242.